

Self-Assembly of *n*-Alkyl- and Aryl-Side Chain Ureas and Their Derivatives as Evidenced by SEM and X-ray Analysis

Oleg V. Kulikov,^{*[a]} Dumindika A. Siriwardane,^[a] Gregory T. McCandless,^[a] Charles Barnes,^[b] Yulia V. Sevryugina,^[c] Joseph D. DeSousa,^[a] Jingbo Wu,^[a] Roger Sommer,^[d] and Bruce M. Novak^{*[a]}

Keywords: Supramolecular chemistry / Self-assembly / Gelation / Nanofibers / Ureas

A small library of ureas and related compounds was synthesized and examined by scanning electron microscopy (SEM), single-crystal X-ray diffraction, powder X-ray (pXRD), and polarized optical microscopy (POM) techniques in order to elucidate the factors controlling their self-assembly in the solid state. Inspection of the 12 solid-state structures revealed that molecules in the crystal lattice are held together by

intermolecular H-bonding, π - π stacking as well as C-H/ π interactions. The same interactions are likely responsible for the formation of supramolecular aggregates (e.g. sheet-like assemblies, micro- and nano-fibers, and the porous networks easily identifiable by SEM technique) and in certain cases led to the small molecules gelation.

Introduction

Simple ureas as well as complex molecules incorporating ureido groups have attracted considerable attention as transmembrane ion transporters,^[1–8] anion receptors,^[9–12] and transdermal penetration enhancers for drug delivery.^[13,14] Besides their well-known ability to form strong intermolecular N–H \cdots O=C hydrogen bonds^[15,16] allowing more efficiently to deliver drugs by amphiphilic block copolymers,^[17a] ureas are of considerable interest for supramolecular polymer chemistry.^[17b] Recent developments are concerned of hydrogen-bonded urea based supramolecular polymers,^[18] which easily undergo intensive intermolecular self-organization process caused by directional H-bonding interactions. Introduction of the urea groups capable of making strong H-bonds in polymer backbone might represent significant interest for multiple potential applications of such nanoribbon/fiberlike morphological systems.^[19–22] Moreover, bis-urea molecules are known to serve as “supramolecular reinforcement fillers” for thermoplastic

elastomers mechanical properties tuning.^[21] Another emerging area of ureas applications is a design of supramolecular LMWGs (low-molecular-weight gelators),^[23] “unimolecular” co-catalysts for cooperative ring-opening polymerization,^[24a] and developing the synthetic foldamers capable to adopt a single screw sense.^[24b–24d] In order to clarify how changes in structure influence the self-assembly properties in the solid state, we prepared and inspected by SEM, powder XRD, polarized optical microscopy (POM), and single-crystal X-ray diffraction analysis a small library of ureas as well as some of their derivatives bearing alkyl substituents varying in length and having different aromatic moieties. We report here the synthesis and morphological characterization of 25 mono-, bis-, tris-ureas as well as bis-carbodiimide and diazetidine (Chart S1). We assume that our structural findings (especially, with regard to the nanofibers) can be used for the potential industrial applications such as design of the materials possessing high non-linear optical anisotropy properties,^[25] creation of degradable polymers for regenerative medicine,^[26] wound debridement,^[27] as promising degradable elastomeric materials for the tissue engineering,^[28] and the development of scaffolds loaded with antibacterial drugs and enzymes.^[29]

Results and Discussion

Synthesis

Synthesis of the ureas of interest was performed by standard techniques (mostly, by condensation of the corresponding amine and isocyanate, ESI vol. 1) in moderate to high yield (Scheme 1).

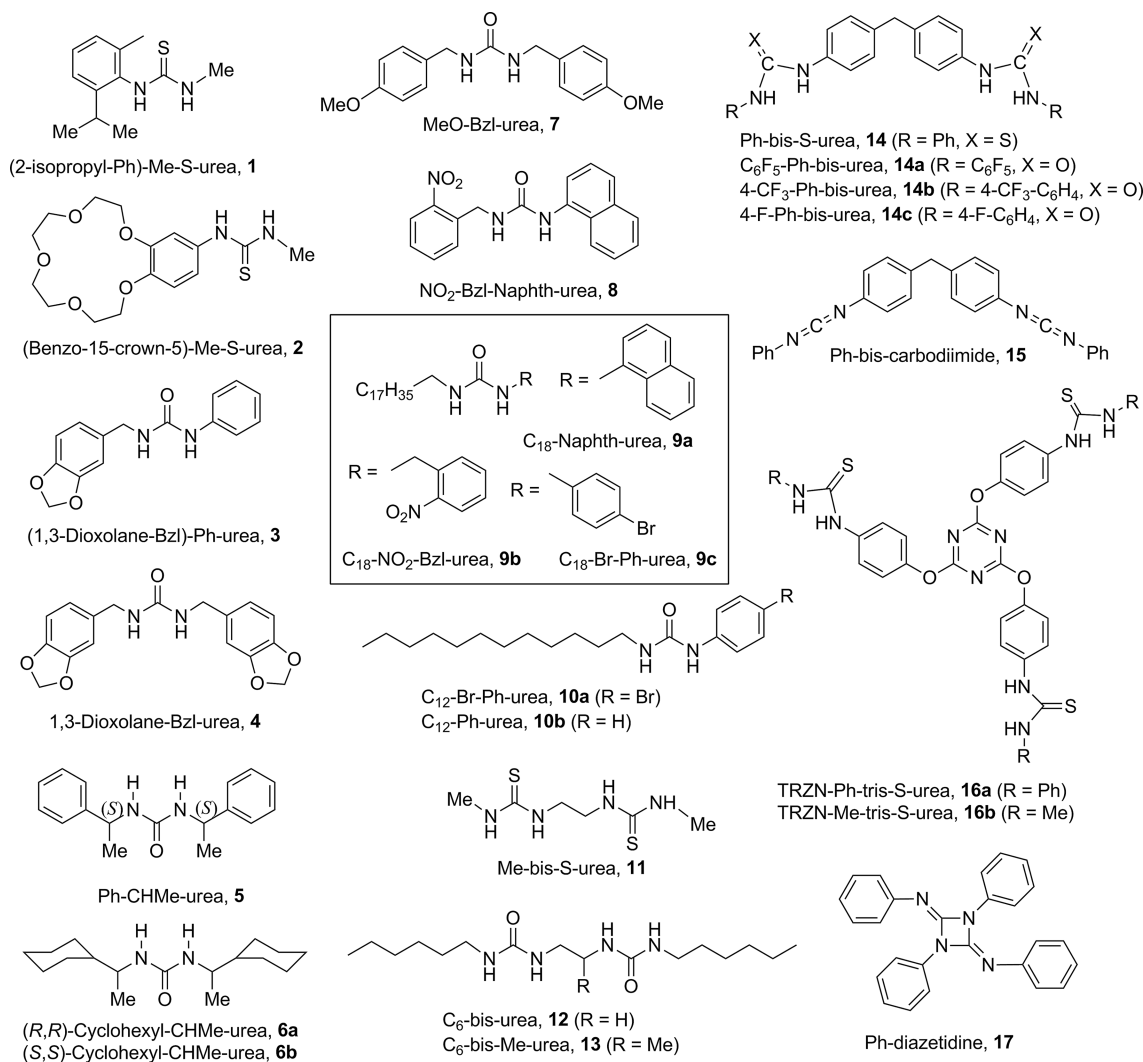
[a] Department of Chemistry, University of Texas at Dallas, Richardson, TX, 75080, USA
E-mail: oleg.kulikov.chem@gmail.com
Bruce.Novak@utdallas.edu
<http://www.utdallas.edu/chemistry/faculty/novak.html>

[b] Department of Chemistry, University of Missouri-Columbia, Columbia, MO, 65211, USA

[c] Department of Chemistry, Texas Christian University, Fort Worth, TX, 76129, USA

[d] Department of Chemistry, North Carolina State University, Raleigh, NC, 27695, USA

Supporting information for this article is available on the WWW under <http://dx.doi.org/10.1002/ejoc.201501242>.



Scheme 1. Structures of ureas and their derivatives used in this study.

X-ray Studies (Single Crystal and Powder pXRD)

Single crystal X-ray studies of target molecules (Figures 1, 2, Supporting Information: S1–S38; Table S1) such as *N*-methyl-*N'*-[2-methyl-6-(1-methylethyl)phenyl]thiourea (**1**); *N*-(benzo-15-crown-5)-*N'*-methylthiourea (**2**); *N*-(1,3-benzodioxol-5-ylmethyl)-*N'*-phenylurea (**3**); *N,N'*-bis(1,3-benzodioxol-5-ylmethyl)urea (**4**); (*S,S*)-*N,N'*-bis(1-phenylethyl)urea (**5**); (*R,R*)-*N,N'*-bis(1-cyclohexylethyl)urea (**6a**); 1,3-bis(4-methoxybenzyl)urea (**7**); *N*-[(2-nitrophenyl)methyl]-*N'*-(1-naphthyl)urea (**8**); *N,N'*-1,2-ethanediyl-bis-*N''*-methylurea (**11**); *N,N'*-1,2-ethanediyl-bis-*N''*-hexylurea (**12**); 4,4'-bis(3-phenylcarbodiimide)diphenylmethane (**15**); 1,3-diphenyl-2,4-diphenylimino-1,3-diazetidene, (**17**) revealed that molecules adopt non-planar conformation and in the crystal lattice interact through intermolecular H-bonding (N–H⋯S=C 2.49, 2.51 Å for **2**, Figure 1, S2; N–H⋯O=C 2.08, 2.22 Å for **3**, Figure S3; 2.03 Å for **4**, Figure S6; 2.08 Å for **5**, Figure S9; 2.13 Å for **6a**, Figure S15; 2.01, 2.05, 2.09, 2.21 Å for **7**, Figure S19; 2.01, 2.18 Å for **8**, Fig-

ure S24; 2.03, 2.04 Å for **12**, Figure S31) or N–H⋯S=C contacts (2.68 Å for **1**, Figure S1; 2.58 Å for **11**, Figure S26) forming 6- and eight-membered patterns. Notably, thiourea **11** represents different polymorph of already known APAJOR^[30] structure developed by Steed lab. It appears that the difference in molecular structure for thiourea **11** and APAJOR is the conformation around terminal C–N bonds. This resulted in dramatic changes in both molecular structure and crystal lattice packing (Figure 1, S27, S28).

We assume that urea molecules form supramolecular aggregates through intermolecular H-bonding as well as π – π stacking and C–H/ π interactions.^[31] The presence of multiple distinct peaks in the powder X-ray diffraction patterns of ureas and their derivatives (Table S2, Figure S40–S50) confirmed high crystallinity of these compounds. The maxima observed probably relate to the interchain distances and layer separation in the crystal lattice.

In particular, reflection peaks at $2\theta \approx 20$ – 30° ($d \approx 4$ – 3 Å) can potentially be attributed to the π – π stacking interaction of the adjacent aromatic fragments. This is in accordance

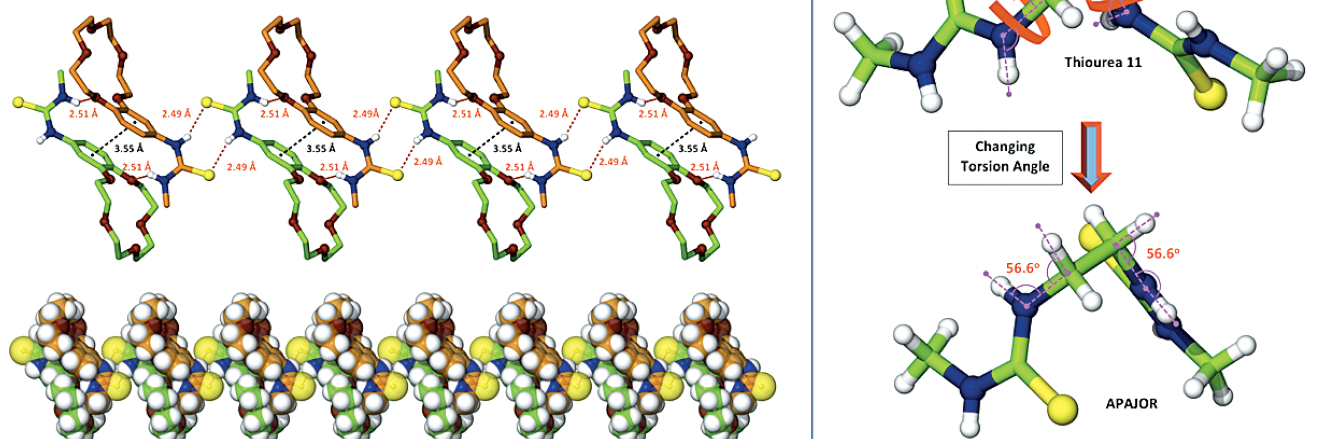


Figure 1. Left side: single-crystal X-ray data (partial crystal packing diagram) for (benzo-15-crown-5)-Me-S-urea (**2**) highlighting intermolecular H-bonding as well as plausible π - π stacking interactions between aromatic rings of the adjacent molecules (non-polar hydrogen atoms are omitted for clarity, space-filling representation is given below); right side: comparison of Me-bis-S-urea (**11**) with its APAJOR (CCDC-795072) conformational isomer.

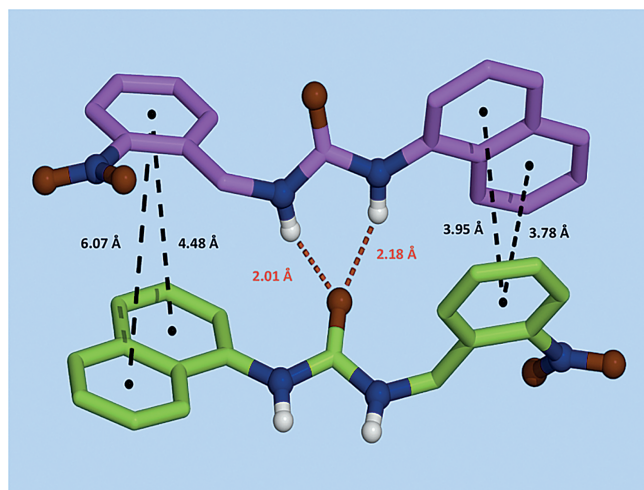


Figure 2. Selected centroid (Ar)⋯centroid (Ar) distances for NO₂-Bzl-Naphth-urea (**8**) (non-polar hydrogen atoms are omitted for clarity).

with single-crystal X-ray data showing plausible π - π and C-H/ π stacking (Figure 1, S2, S4, S20, S22–S24, S33). However, in certain cases (Figure S1, S3, S6, S9, S19, S36), intermolecular distances between aromatic rings are significantly longer than the currently accepted maximum distance for π - π interactions. Thus, urea **8** exhibited the distance between the ring centroids 3.78, 3.95 Å and 4.48, 6.07 Å, correspondingly (Figure 2). Notably, along with the hydrogen bonding interactions of the ureido group (e.g. –NH–CO–NH–), between neighboring molecules of **8**, the packing conformation along the crystallographic “*a*” direction can be described as “head-to-tail” (with nitrophenyl group as the “head” and the naphthyl group as the “tail”)

as well as a “zig-zag” (with intermolecular dihedral angles of the ureido group alternating between approximately +47.7° and –47.7°). Figure 2, S24 display this alternating structural arrangement. Plausible intermolecular π - π interactions between nitrophenyl and naphthyl groups with centroid-to-centroid distance of 3.78, 3.95 Å and dihedral angle of ca. 5.2° have been identified. This interaction is confined to “pairs” since the next neighboring molecule will have a dihedral angle equal in magnitude, but opposite in direction (a part of the “zig-zag” packing pattern), and, therefore, a longer separation distances (4.48, 6.07 Å). The intramolecular dihedral angle between the nitrophenyl and naphthyl groups is ca. 68.6°. Our rationale for the use of urea **8** was that introducing naphthyl moiety would possibly increase π - π stacking if compared with the other aromatic ureas in this study (e.g. ureas **1–5**, **7**) not having fused aromatic rings. Similarly, the presence of four aromatic fragments in the structure of carbodiimide **15** would likely enhance π - π interactions between the adjacent molecules resulting in formation of the supramolecular stack (Figure 3, left panel). The same kind of “ π - π enforcement” could be achieved by appending three hydrogen-bonding thiourea moieties to triazine core in urea **16a** structure (Figure 3, right panel). Presumably, individual tris-urea **16a** molecules in hypothetical stack are held together by combination of hydrogen bonds between thiourea groups as well as π - π interactions of seven aromatic rings.

We should also note that Ph-CHMe-urea (**5**) (Figure S9) has been previously reported (EFETEQ, CCDC-978481). The known structure (CCDC-978481) and urea **5** are nearly identical. In both cases the molecule sits on a twofold axis through the C=O bond. As expected, the anomalous dispersion refinement of the Flack parameter determined for urea **5** points to the correct absolute configuration.^[32]

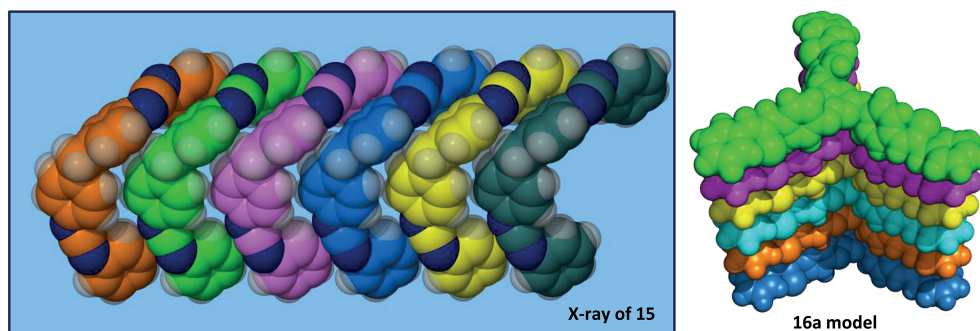


Figure 3. Single crystal X-ray data (partial crystal packing diagram) for Ph-bis-carbodiimide **15** (left) and hypothetical stack of TRZN-Ph-tris-S-urea (**16a**) (right).

Morphology Studies by SEM and Gelation Behavior

We hypothesize that intermolecular hydrogen bonding as well as the other types of non-covalent weak interactions revealed by X-ray studies are responsible for organizing urea molecules into supramolecular aggregates that could be visualized by SEM and POM techniques. Inspection of ureas by SEM showed great variety of morphologies such as fibers, plate-like aggregates, porous networks, rod-like assemblies, etc. (Figures 4, 5, 6, and 7, Supporting Information: 2S1–2S108; Table 2S1).

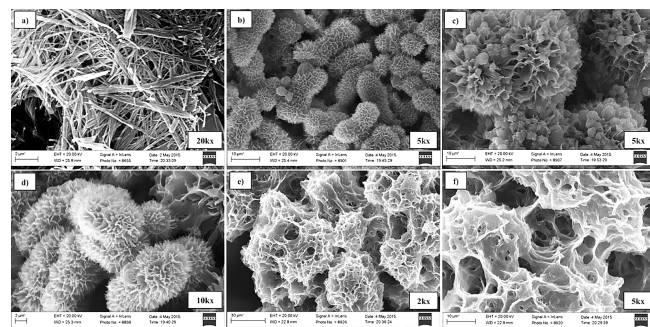


Figure 4. SEM images of C_6 -bis-Me-urea (**13**) as a solid obtained by crystallization from DMF (panel a); C_{18} -Br-Ph-urea (**9c**) deposited from THF, 66 mg/mL (panels b–d); C_{18} -NO₂-Bzl-urea (**9b**) deposited from THF, 66 mg/mL (panels e, f).

Micrographs of bis-urea **13** (Figure 4, a, Supporting Information: 2S65–2S71) displayed clearly identifiable fibrillar network patterns that were presumably formed due to the bundling of individual urea fibers when prepared the specimen by crystallization from different solvents including EtOH (2S65, 2S66), DMF (2S67–2S71). Patterns observed are typical in appearance for most of the images collected for ureas in this study as well as for their derivatives. Inspection of the ureas **9c** and **9b** deposited from the high concentration stock solutions (THF, 66 mg/mL) revealed interesting porous self-assembled morphologies (Figure 4, b–f, Supporting Information: 2S39–2S41, 2S44–2S48). It seems likely that, due to the conformational freedom of the flexible octadecyl substituents in both ureas, hydrophobic pockets could be formed where solvent molecules are entrapped and, therefore, decreasing the crystallinity of material comparative to their short chain homologous struc-

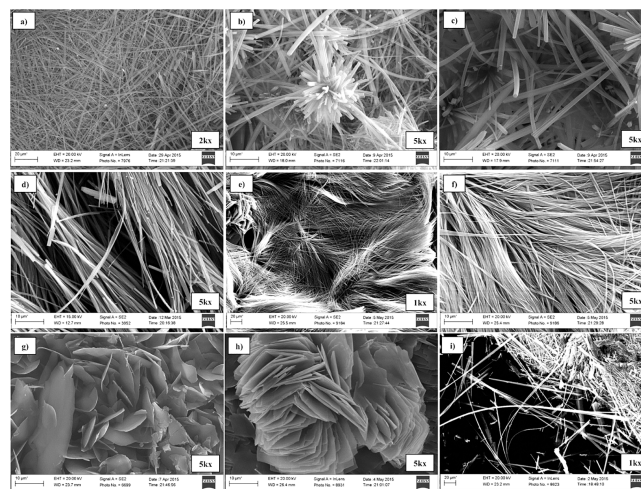


Figure 5. SEM images of NO₂-Bzl-Naphth-urea (**8**) deposited from 1,4-dioxane, 33 mg/mL (panel a); urea **8** deposited from THF, 22 mg/mL (panels b, c); (1,3-dioxolane-Bzl)-Ph-urea (**3**) as a solid obtained by crystallization from EtOH (panel d); urea **3** deposited from THF, 66 mg/mL (panels e, f); Ph-bis-S-urea (**14**) obtained by precipitation from EtOAc/MeOH (panel g); C_{12} -Ph-urea (**10b**) deposited from THF, 66 mg/mL (panel h); C_{12} -Br-Ph-urea (**10a**) as a solid obtained by crystallization from EtOAc/EtOH (panel i).

tures. As a result of losing THF molecules during solvent evaporation, large cavities could be generated that is clearly seen in the panels of Figure 4, c and f, Supporting Information: 2S41, 2S46. Changing the solvent system dramatically effects molecules self-organization. Thus, **9c** (when crystallized from the mixture EtOH/CHCl₃) produced randomly oriented fibers that fuse and split forming network (Figure 2S42, 2S43). Detailed morphological features of the self-assembled aggregates based on long-chain tris-ureas (e.g. dodecyl and octadecyl) have been recently communicated.^[33a,33b] Reversible tris-urea gelators incorporating phenylureido groups similar to **16a** structure have been synthesized and inspected by SEM.^[33c] Randomly oriented fibers are apparent in the panels a–c of the Figure 5 displaying self-assembled morphologies derived from urea **8** with estimated bent fiber width ≥ 300 nm (1,4-dioxane, Figure 2S27b) and ≥ 200 nm (THF, Figure 2S31c).

Use of EtOH as a solvent for urea **8** crystallization allowed to acquire images of shorter rod-like aggregates (Fig-

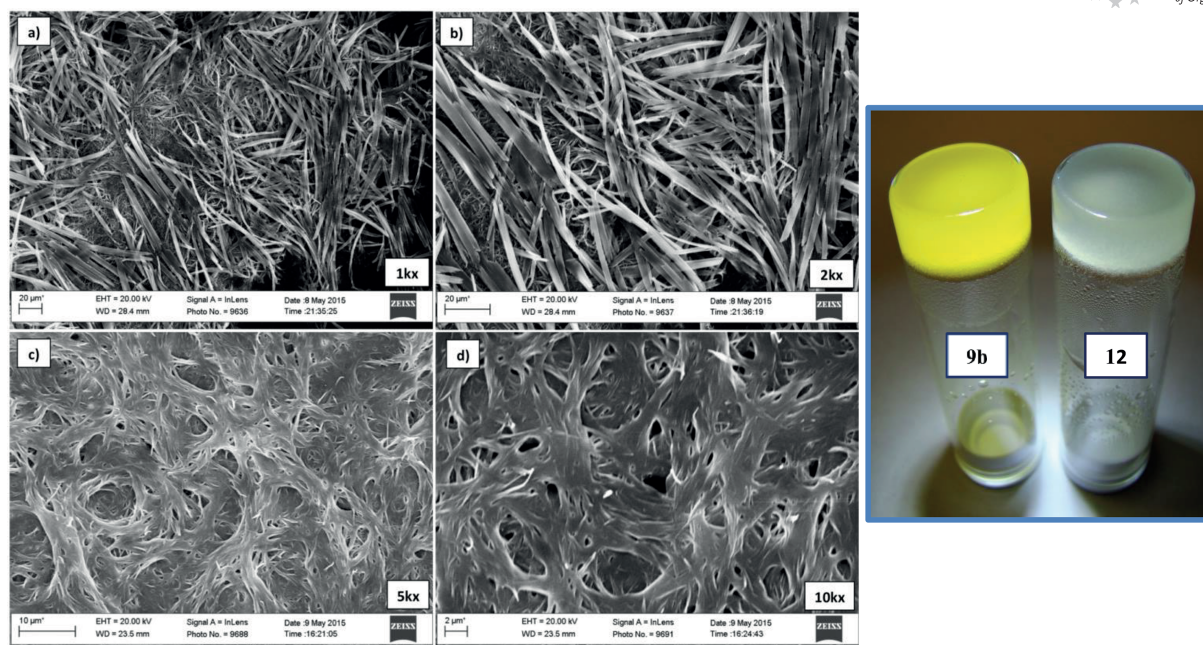


Figure 6. SEM images of the dried gels of C_6 -bis-urea (**12**) (panels a, b) and C_{18} -NO₂-Bzl-urea (**9b**) (panels c, d) deposited from PhNO₂, 66 mg/mL.

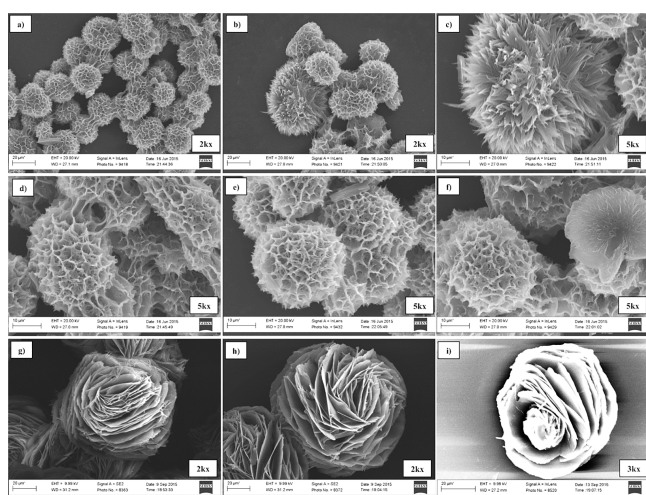


Figure 7. SEM images of the dried gels of C_{18} -NO₂-Bzl-urea (**9b**) (panels a–f) deposited from CHCl₃, 20 mg/mL and 4-F-Ph-bis-urea (**14c**) deposited from the hot DMF stock solution, 80 mg/mL (panels g–i).

ures 2S32–2S34) thus implying that solvent choice has an effect on self-assembly in the solid state. More morphologies of this nature have been deposited in ESI, vol. 2 (Figures 2S24–2S34). Figure 5 (d–f) showed uniform bundled fibrous aggregates of urea **3** depending on solvent – (EtOH, panel d) and THF (panels e, f). Drop cast deposition from THF stock solution (66 mg/mL) displays clearly identifiable nanofibers (ca. 600 nm in width, Figure 2S4–2S8) that at high magnification (5, 10 k \times) appear to be the clusters of ribbon-like aggregates (Figure 2S8a–c). Again, changing the solvent (e.g. THF to EtOH) and the sample preparation caused noticeable changes in appearance – short rod-like

aggregates became the predominant motif (Figure 2S9–11). Lower row panels g–i of the Figure 5 demonstrate aggregated planar sheets and very distinct fibrous structures obtained from urea **14** as well as long-chain ureas **10a** and **10b** bearing dodecyl substituent. Additional SEM micrographs displaying fibrillary morphologies/plate-like aggregates for compounds **10a**, **10b** and **14** could be found in Figure 2S50–2S60, 2S72–2S76. Importantly, well-defined plates organized into 3D-network and having thickness ranging from 348 nm to 477 nm could be observed in the panels of Figure 2S76 (urea **14**), whereas **10b** demonstrated pretty dense plate packing arrangement (280–661 nm in thickness for the individual plates, Figure 2S58). Notably, deposition of urea **10b** from THF stock (66 mg/mL) resulted in formation of quite unusual rose-like aggregates (Figure 5, h, Figure 2S60). These observations are in accordance with the previous results from Hamilton lab^[34] detailing the synthesis and self-assembly properties of polymerizable organogelators and the low molecular weight gelators incorporating ureido moieties. Also, the recent contributions to urea-based supramolecular gels^[23,35] area should not be underestimated.

Despite the fact that gelation is not the focus of current work, we decided to inspect aggregation behaviour of selected ureas in order to evaluate their propensity to form gels using the same solvent, concentration, and SEM sample preparation method (Figure 2S93–2S108, Table 2S2). Compounds **8**, **9a–9c**, **10a**, **10b**, **12**, and **13** have been found to form organogels when their respective stock solutions in the nitrobenzene (66 mg/mL) were cooled down to the room temperature (Figure 2S93). Importantly, urea **10b** having relatively short dodecyl aliphatic chain produced leaking gel, while model urea **11** with terminal methyl groups found to be soluble in the nitrobenzene with no gel-

ling at the ambient temperature. Other seven ureas tested clearly demonstrated formation of the slightly turbid stable gels upon cooling. This is not unexpected since longer alkyl chains (C_{18} - vs. C_{12} - and methyl in case of urea **11**) as well as the presence of two ureido groups in one molecule in case of compounds **12** and **13** should facilitate the gel formation. Evidently, naphthyl group in compounds **8** and **9a** might assist effective gelation too due to the increased ability to form supramolecular π - π stacks. Nitrobenzene was selected for a gel testing because of its high boiling point and, as a consequence, low volatility, although ureas gelation was detected in some other solvents such as $CHCl_3$ and DMSO as well (Figure 2S85–2S92). Also, all ureas tested showed good solubility in the nitrobenzene at high concentration when heated, unlike the other solvents. The latter appears to be highly important to prepare SEM specimens under the same experimental conditions for comparison purpose. SEM inspection of the dried gels exhibited similarly looking fibrous motifs (Figure 6, 2S94–2S108).

Figure 6 demonstrated aggregates obtained from ureas **9b** and **12** when dissolved in the nitrobenzene and cooled down to the room temperature. Panels a and b showed no meaningful differences compared to the previously described fiber-like structures, whereas panels c and d both depicted not well resolved intertwining bundles of fibers as the major morphological feature of compound **9b**. This may be indicative of low crystallinity of **9b** that was also evidenced by the corresponding pXRD profile (Figure S50). Interestingly, the presence of octadecyl alkyl chain promotes the formation of spherical sponge-like aggregates (Figure 7, a–f, 2S86–2S89). Again, the latter phenomenon the best could be explained by liberating $CHCl_3$ molecules from hydrophobic pockets formed by long aliphatic chains during specimen preparation.

In general, analysing the library of SEM images collected for mono-, bis- and tris-ureas as well as their derivatives (bis-carbodiimide **15** and the product of diphenylcarbodiimide dimerization – diazetidine **17**), we infer that depending on structure and solvent used for the sample preparation, molecules of the tested compounds tend to form diverse morphologies with predominance of rod-like and fiber-like aggregates. Although the use of mono-ureas may

be considered as over-simplification in terms of their ability to form extensive hydrogen bonding and π -stacking motifs comparatively to their bis- and tris-urea analogues, most of them exhibited very distinctively looking morphologies when examined by SEM.

In addition to that, we have studies morphologies assembled from fluorinated bis-ureas (**14a–14c**, Figure 7, g–i, 3S1–3S22, Table 3S1) in order to elucidate the role of strong electron-withdrawing substituents in aggregation behaviour. Interestingly, compound 4-F-Ph-bis-urea (**14c**) tends to form rose-like aggregates when deposited from the hot DMF stock solution on the glass slide (cold deposition of the same bis-urea yielded less ordered sheet-like aggregates, Figure 3S17). Somewhat similar was observed for 4- CF_3 -Ph-bis-urea (**14b**), e.g. plate-like aggregates are clearly visible in the panels of Figures 3S9 and 3S10. We assume that along with classical intermolecular $N-H\cdots O=C$ hydrogen bonding, weak $C_{aryl}-H\cdots F$ interactions of the adjacent molecules or even $C-F\cdots C=O$ orthogonal interactions^[36a] might be involved in determining the orientation of fluorinated urea molecules with respect to each other and, consequently, resulting in formation of these unusual supramolecular assemblies, however this is not clear enough to be convincing. All fluorinated ureas were found to form gels in either DMF or $PhNO_2$ at 80 mg/mL, moreover C_6F_5 -bis-urea (**14a**) bearing perfluorinated pendant groups seemed to be the strongest gelator capable of producing stiff transparent supramolecular gel (Figure 3S6–3S8, 3S18, 3S19) in both solvents.

Polarized Optical Microscopy (POM) Studies

The polarized optical microscopy images have been recorded for certain ureas (Figures 8, 9, 2S109–2S123) showing magnificent birefringent textures and rod-like aggregates indicative of formation the highly ordered, crystalline domains as a result of self-assembly.

Figure 8 displayed crystalline arrangements obtained from the ureas **1** and **5** in THF. Interestingly, mono-urea **1** failed to provide visible images under polarized light at typical concentration range used (22–66 mg/mL), probably as a result of very high solubility in this particular solvent

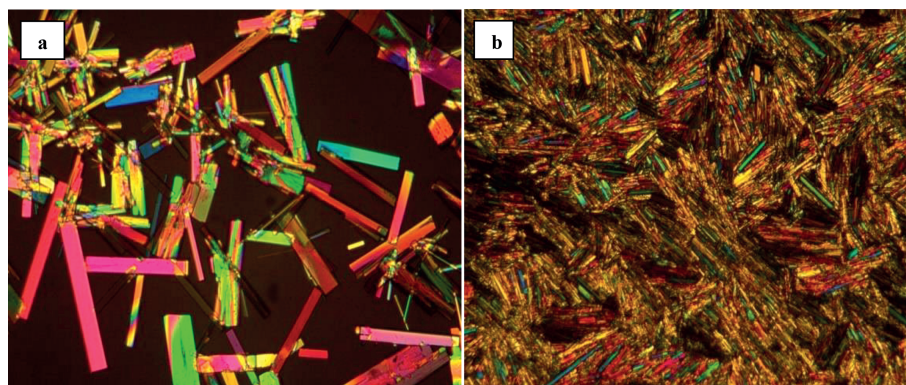


Figure 8. POM micrographs ($10\times$) of (2-isopropyl-Ph)-Me-S-urea (**1**) deposited from THF, 560 mg/mL (a); Ph-CHMe-urea (**5**) deposited from THF, 33 mg/mL (b).

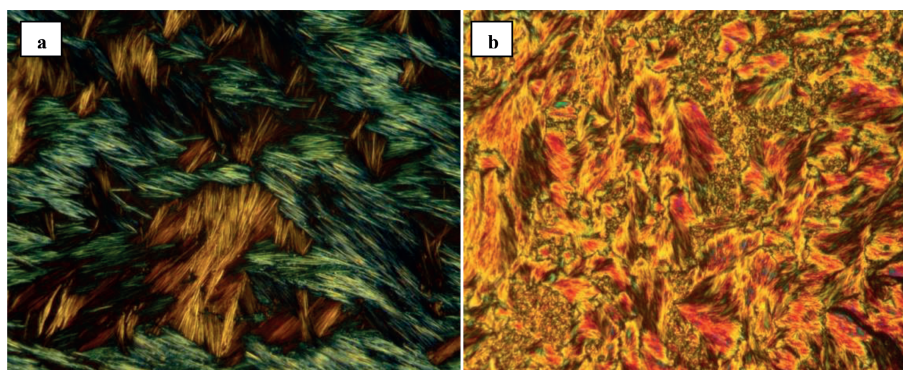


Figure 9. POM micrographs (10 \times) of NO₂-Bzl-Naphth-urea (**8**) deposited from 1,4-dioxane, 33 mg/mL (panel a) and from PhNO₂, 66 mg/mL, gel (panel b).

(THF). Nevertheless, high concentration stock solution (560 mg/mL) could be used to generate the images of rod shaped structures (Figure 8, a, 2S120), thus providing unambiguous evidence for urea liquid crystalline properties.^[34a,36b,36c] Similarly, bis-urea **11** formed aggregates (Figure 2S122) when deposited from PhNO₂ stock solution (66 mg/mL) in the form of crystals that are markedly smaller than motifs depicted on the panel a of Figure 8. Also, urea **10b** colourful textures (Figure 2S123) found to be collapsible into crystalline network upon specimen aging (ca. 1 month) as shown in Figure 2S124. Figure 9 showed POM images of urea **8** acquired in 1,4-dioxane (panel a) and nitrobenzene (panel b). These observations are consistent with rectangular/hexagonal columnar liquid crystal superstructures discovered for mono-urea molecules bearing C₈-, C₁₂-, and C₁₆-substituents.^[36b]

Conclusions

In summary, a small family of simple ureas as well as compounds derived from them, has been synthesized and inspected by combination of single-crystal X-ray diffraction analysis, powder XRD, SEM, and POM techniques. Urea molecules proved to self-assemble in the solid state into various aggregates and this process is likely driven by hydrogen bonding, π - π , and C-H/ π -stacking interactions of the adjacent molecules aromatic moieties as evidenced by X-ray diffraction analysis. For the ureas bearing either alkyl side chains or fluorinated substituents, the other factors such as hydrophobic side chain/side chain interactions and/or non-classical C_{aryl}-H \cdots F and C-F \cdots C=O orthogonal interactions should not be underestimated since they help stabilize molecules in supramolecular network. This is especially pronounced in ureas bearing multiple fluorine atoms, thus effecting self-association of individual molecules and, consequently, gelation. At least seven out of eight non-fluorinated ureas tested in the nitrobenzene (**8**, **9a–9c**, **10a**, **10b**, **12**, and **13**) clearly exhibited gelating ability. The morphologies observable by SEM and POM techniques are believed to be directly related to the aforementioned non-covalent interactions leading to the formation of supramolecular aggregates. Also, introducing additional ureido moieties/aromatic fragments would likely enhance π - π

stacking propensity allowing to control aggregation in ureas. Another important finding was the morphological changes have occurred upon changing the solvent, concentration, and deposition temperature that might be employed to grow specific motifs (e.g. needle-like aggregates, bent fibers, ribbons, rose-like plates, etc.). These urea-based morphologies might be applicable for designing the novel functional materials.

Experimental Section

General Methods: All starting materials used were obtained from Sigma–Aldrich, Fluka or TCI America and were used without further purification unless otherwise noted. Thin-layer chromatography (TLC) was performed on Sigma–Aldrich TLC Plates (silica gel on aluminum, 200 mm layer thickness, 2–25 mm particle size, 60 Å pore size). ¹H nuclear magnetic resonance spectra were recorded either on Bruker Avance IITM 500 instrument at 500 MHz or Mercury 400BB at 400 MHz. ¹³C NMR spectra were recorded on the same instruments at 125 MHz and 100 MHz, correspondingly. ¹H and ¹³C chemical shifts are reported in parts per million (ppm) relative to the corresponding residual solvent peak. High-resolution electrospray mass spectra (HR-ESI MS) were obtained on Agilent technologies 6530 Accurate Mass QT of LC/MS instrument at University of Texas at Austin, Chemistry Department Mass Spectrometry Facility. Powder X-ray diffraction (pXRD) data profiles were recorded on Rigaku Ultima III XRD diffractometer (Nano Characterization Facility at UTD).

Supporting Information (see footnote on the first page of this article): Experimental procedures, spectroscopic data for all novel ureas as well as single-crystal X-ray diffraction data can be found.

Acknowledgments

Funding of this work was provided by the Faculty start-up fund from the University of Texas at Dallas (UTD) and the Endowed Chair for Excellence at UTD. We wish to thank Mr. Kyle Johnson for the preparation of urea **2**. We gratefully acknowledge the National Science Foundation (NSF) (NSF-MRI grantCHE-1126177) used to purchase the Bruker Avance III 500 NMR instrument.

- [1] S. J. Moore, M. Wenzel, M. E. Light, R. Morley, S. J. Bradberry, P. Gomez-Iglesias, V. Soto-Cerrato, R. Perez-Tomas, P. A. Gale, *Chem. Sci.* **2012**, 3, 2501–2509.

- [2] S. J. Moore, C. J. E. Haynes, J. Gonzalez, J. L. Sutton, S. J. Brooks, M. E. Light, J. Herniman, G. J. Langley, V. Soto-Cerrato, R. Perez-Tomas, I. Marques, P. J. Costa, V. Felix, P. A. Gale, *Chem. Sci.* **2013**, *4*, 103–117.
- [3] N. J. Andrews, C. J. E. Haynes, M. E. Light, S. J. Moore, C. C. Tong, J. T. Davis, W. A. Harrell Jr., P. A. Gale, *Chem. Sci.* **2011**, *2*, 256–260.
- [4] C. J. E. Haynes, S. J. Moore, J. R. Hiscock, I. Marques, P. J. Costa, V. Felix, P. A. Gale, *Chem. Sci.* **2012**, *3*, 1436–1444.
- [5] N. Busschaert, S. J. Bradberry, M. Wenzel, C. J. E. Haynes, J. R. Hiscock, I. L. Kirby, L. E. Karagiannidis, S. J. Moore, N. J. Wells, J. Herniman, G. J. Langley, P. N. Horton, M. E. Light, I. Marques, P. J. Costa, V. Felix, J. G. Frey, P. A. Gale, *Chem. Sci.* **2013**, *4*, 3036–3045.
- [6] H. Valkenier, C. J. E. Haynes, J. Herniman, P. A. Gale, A. P. Davis, *Chem. Sci.* **2014**, *5*, 1128–1134.
- [7] M. J. Spooner, P. A. Gale, *Chem. Commun.* **2015**, *51*, 4883–4886.
- [8] a) N. Busschaert, L. E. Karagiannidis, M. Wenzel, C. J. E. Haynes, N. J. Wells, P. G. Young, D. Makuc, J. Plavec, K. A. Jolliffe, P. A. Gale, *Chem. Sci.* **2014**, *5*, 1118–1127; b) E. B. Park, K. Jeong, *Chem. Commun.* **2015**, *51*, 9197–9200; c) L. E. Karagiannidis, C. J. E. Haynes, K. J. Holder, I. L. Kirby, S. J. Moore, N. J. Wells, P. A. Gale, *Chem. Commun.* **2014**, *50*, 12050–12053.
- [9] P. A. Gale, J. R. Hiscock, C. Z. Jie, M. B. Hursthouse, M. E. Light, *Chem. Sci.* **2010**, *1*, 215–220.
- [10] J. P. Clare, A. Statnikov, V. Lynch, A. L. Sargent, J. W. Sibert, *J. Org. Chem.* **2009**, *74*, 6637–6646.
- [11] M. P. Hughes, B. D. Smith, *J. Org. Chem.* **1997**, *62*, 4492–4499.
- [12] a) M. Wenzel, M. E. Light, A. P. Davis, P. A. Gale, *Chem. Commun.* **2011**, *47*, 7641–7643; b) Y. Liu, K. Yuan, L. Lv, Y. Zhu, Z. Yuan, *J. Phys. Chem. A* **2015**, *119*, 5842–5852; c) N. Mittal, K. M. Lippert, C. K. De, E. G. Klauber, T. J. Emge, P. R. Schreiner, D. Seidel, *J. Am. Chem. Soc.* **2015**, *137*, 5748–5758; d) I. L. Kirby, M. B. Pitak, C. Wilson, P. A. Gale, S. J. Coles, *CrystEngComm* **2015**, *17*, 2815–2826; e) M. Olivari, R. Montis, L. E. Karagiannidis, P. N. Horton, L. K. Mapp, S. J. Coles, M. E. Light, P. A. Gale, C. Caltagirone, *Dalton Trans.* **2015**, *44*, 2138–2149; f) N. Busschaert, C. Caltagirone, W. V. Rossum, P. A. Gale, *Chem. Rev.* **2015**, *115*, 8038–8155.
- [13] D. A. Godwin, M. R. Player, J. W. Sowell, B. B. Michniak, *Int. J. Pharm.* **1998**, *167*, 165–175.
- [14] S. G. Lee, S. R. Kim, H. I. Cho, M. H. Kang, D. W. Yeom, S. H. Lee, S. Lee, Y. W. Choi, *Biol. Pharm. Bull.* **2014**, *37*, 1674–1682.
- [15] M. C. Etter, Z. Urbanczyk-Lipkowska, M. Zia-Ebrahimi, T. W. Panunto, *J. Am. Chem. Soc.* **1990**, *112*, 8415–8426.
- [16] L. Li, Z. Fei, X. Meng, L. Cao, T. Pang, Y. Zhu, A. Wu, *Struct. Chem.* **2013**, *24*, 97–104.
- [17] a) J. P. K. Tan, S. H. Kim, F. Nederberg, K. Fukushima, D. J. Coady, A. Nelson, Y. Y. Yang, J. L. Hedrick, *Macromol. Rapid Commun.* **2010**, *31*, 1187–1192; b) L. Yang, X. Tan, Z. Wang, X. Zhang, *Chem. Rev.* **2015**, *115*, 7196–7239.
- [18] J. Swiergiel, L. Bouteiller, J. Jadzyn, *Macromolecules* **2014**, *47*, 2464–2470.
- [19] N. E. Botterhuis, S. Karthikeyan, D. Veldman, S. C. J. Meskers, R. P. Sijbesma, *Chem. Commun.* **2008**, 3915–3917.
- [20] E. Wisse, A. J. H. Spiering, F. Pfeifer, G. Portale, H. W. Siesler, E. W. Meijer, *Macromolecules* **2009**, *42*, 524–530.
- [21] a) E. Wisse, L. E. Govaert, H. E. H. Meijer, E. W. Meijer, *Macromolecules* **2006**, *39*, 7425–7432; b) E. Wisse, A. J. H. Spiering, P. Y. W. Dankers, B. Mezari, P. C. M. M. Magusin, E. W. Meijer, *J. Polym. Sci., Part A: Polym. Chem.* **2011**, *49*, 1764–1771.
- [22] R. A. Koevoets, R. M. Versteegen, H. Kooijman, A. L. Spek, R. P. Sijbesma, E. W. Meijer, *J. Am. Chem. Soc.* **2005**, *127*, 2999–3003.
- [23] L. Meazza, J. A. Foster, K. Fucke, P. Metrangolo, G. Resnati, J. W. Steed, *Natur. Chem.* **2013**, *5*, 42–47.
- [24] a) O. I. Kazakov, P. P. Datta, M. Isajani, E. T. Kiesewetter, M. K. Kiesewetter, *Macromolecules* **2014**, *47*, 7463–7468; b) R. Wehchel, J. Maury, J. Fremaux, S. P. France, G. Guichard, J. Clayden, *Chem. Commun.* **2014**, *50*, 15006–15009; c) J. Fremaux, C. Dolain, B. Kauffmann, J. Clayden, G. Guichard, *Chem. Commun.* **2013**, *49*, 7415–7417; d) J. Clayden, L. Lemiegre, G. A. Morris, M. Pickworth, T. J. Snape, L. H. Jones, *J. Am. Chem. Soc.* **2008**, *130*, 15193–15202.
- [25] D. Isakov, E. M. Gomes, M. Belsley, B. Almeida, A. Martins, N. Neves, R. Reis, *Europhys. Lett.* **2010**, *91*, 28007-p1–28007-p4.
- [26] F. Lin, J. Yu, W. Tang, J. Zheng, S. Xie, M. L. Becker, *Macromolecules* **2013**, *46*, 9515–9525.
- [27] E. Shoba, R. Lakra, M. S. Kiran, P. S. Korrapati, *RSC Adv.* **2014**, *4*, 60209–60215.
- [28] E. Borg, A. Frenot, P. Walkenstrom, K. Gisselalt, C. Gretzer, P. Gatenholm, *J. Appl. Polym. Sci.* **2008**, *108*, 491–497.
- [29] A. Diaz, L. J. Valle, D. Tugushi, R. Katsarava, J. Puiggali, *Mater. Sci. Eng. C* **2015**, *46*, 450–462.
- [30] J. T. Lenthall, J. A. Foster, K. M. Anderson, M. R. Probert, J. A. K. Howard, J. W. Steed, *CrystEngComm* **2011**, *13*, 3202–3212.
- [31] a) M. Nishio, *CrystEngComm* **2004**, *6*, 130–158; b) E. A. Meyer, R. K. Castellano, F. Diederich, *Angew. Chem. Int. Ed.* **2003**, *42*, 1210–1250; *Angew. Chem.* **2003**, *115*, 1244–1287; c) C. A. Hunter, K. R. Lawson, J. Perkins, C. J. Urch, *J. Chem. Soc. Perkin Trans. 2* **2001**, 651–669.
- [32] Originally, the data set for urea **5** was collected by using Mo radiation ($\lambda = 0.7107 \text{ \AA}$), however, since Cu source ($\lambda = 1.5418 \text{ \AA}$) offers considerably stronger anomalous dispersion that is essential for absolute configuration determination, the final data set reported here represents Cu data only. The value for the Flack parameter is 0.12(2), and it is believed that this value would be considered to be a strong support of the proposed absolute configuration (e.g., *S,S*-configuration) of the urea **5**.
- [33] a) C.-C. Lu, S.-K. Su, *J. Chin. Chem. Soc.* **2009**, *56*, 121–126; b) C.-C. Lu, S.-K. Su, *J. Chin. Chem. Soc.* **2009**, *56*, 115–120; c) M. Yamanaka, T. Nakamura, T. Nakagawa, H. Itagaki, *Tetrahedron Lett.* **2007**, *48*, 8990–8993.
- [34] a) G. Wang, A. D. Hamilton, *Chem. Eur. J.* **2002**, *8*, 1954–1961; b) G. Wang, A. D. Hamilton, *Chem. Commun.* **2003**, 310–311; c) L. A. Estroff, A. D. Hamilton, *Chem. Rev.* **2004**, *104*, 1201–1217; d) C. Shi, Z. Huang, S. Kilic, J. Xu, R. M. Enick, E. J. Beckman, A. J. Carr, R. E. Melendez, A. D. Hamilton, *Science* **1999**, *286*, 1540–1543.
- [35] a) F. Piana, M. Facciotti, G. Pileio, J. R. Hiscock, W. V. Rossum, R. C. D. Brown, P. A. Gale, *RSC Adv.* **2015**, *5*, 12287–12292; b) M. Loos, A. Friggeri, J. Esch, R. M. Kellogg, B. L. Feringa, *Org. Biomol. Chem.* **2005**, *3*, 1631–1639; c) F. S. Schoonbeek, J. H. Esch, R. Hulst, R. M. Kellogg, B. L. Feringa, *Chem. Eur. J.* **2000**, *6*, 2633–2643; d) J. Rubio, V. Marti-Centelles, M. I. Burguete, S. V. Luis, *Tetrahedron* **2013**, *69*, 2302–2308; e) J. A. Foster, D. W. Johnson, M.-O. M. Pipenbrock, J. W. Steed, *New J. Chem.* **2014**, *38*, 927–932; f) J. A. Foster, R. M. Edkins, G. J. Cameron, N. Colgin, K. Fucke, S. Ridgeway, A. G. Crawford, T. B. Marder, A. Beeby, S. L. Cobb, J. W. Steed, *Chem. Eur. J.* **2014**, *20*, 279–291; g) M.-O. M. Pipenbrock, N. Clarke, J. A. Foster, J. W. Steed, *Chem. Commun.* **2011**, *47*, 2095–2097.
- [36] a) E. Persch, O. Dumele, F. Diederich, *Angew. Chem. Int. Ed.* **2015**, *54*, 3290–3327; b) B. Glettner, S. Hein, R. A. Reddy, U. Baumeister, C. Tschierske, *Chem. Commun.* **2007**, 2596–2598; c) K. Kishikawa, S. Nakahara, Y. Nishikawa, S. Kohmoto, M. Yamamoto, *J. Am. Chem. Soc.* **2005**, *127*, 2565–2571.

Received: September 28, 2015

Published Online: October 28, 2015